Stimulated-Raman-scatter behavior in a relativistically hot plasma slab and an electromagnetic low-order pseudocavity

A. Ghizzo,[1] T. W. Johnston,[2] T. Réveillé,[1] P. Bertrand,[1] and M. Albrecht-Marc[1]
[1]*L.P.M.I.A., Université Henri Poincaré, Boîte Postale 239, 54506 Vandoeuvre les Nancy Cedex, France*
[2]*I.N.R.S. Energie, Matériaux et Télécommunications, Case Postal 1020, Varennes, Quebec, Canada J3X1S2*
(Received 30 November 2005; revised manuscript received 2 June 2006; published 18 October 2006)

Particle simulations on a flat-topped somewhat underdense (typically $n_0/n_c=0.6$) plasma slab by Nikolic *et al.* [Phys. Rev. E **66**, 036404 (2002)] were seen to give transient stimulated scattering behavior with frequency shift $[\omega_0-\omega_s(\approx\omega_p)]$ considerably less than the plasma frequency ω_p. This has been linked to the electron acoustic wave (EAW) and the scattering was thus seen as another example of stimulated electron acoustic scattering inferred by Montgomery *et al.* [Phys. Rev. Lett. **87**, 155001 (2001)] from experiments on low-density plasmas. Montgomery *et al.* had noted the difficulty of how one could have a very narrow observed scattering from a wave whose damping was at least initially very high. Our Vlasov-Maxwell simulations for such somewhat underdense ($n_0/n_c\geqslant 0.25$) plasmas show that the simulation resonance was in fact determined by the beating of the pump with a new "radiating pseudocavity" electromagnetic mode for the slab at a frequency close to ω_p with relatively low loss. This allows the initial narrow-band excitation of the kinetic electrostatic electron nonlinear (KEEN) waves (the nonlinear "cousins" of EAWs) at a well-defined frequency ($\omega_K\approx\omega_0-\omega_p<\omega_p$) which is not necessarily the value given by the EAW dispersion relation. (The KEEN wave characteristics have been discussed by Afeyan *et al.* [33rd AAAC (2003), #238, IFSA 2003].) The consideration of such a mechanism is relevant to moderately underdense hot plasmas.

DOI: 10.1103/PhysRevE.74.046407 PACS number(s): 52.35.Mw, 52.25.Dg, 52.35.Sb, 52.38.Dx

I. INTRODUCTION

Particle-in-cell (PIC) simulation work has been recently published by Nikolic, Skoric, Ishiguro and Sato [1] (referred to hereafter as NSIS) using the interaction of very intense (near to being electron-relativistic) laser light with a moderately dense plasma slab ($n_0/n_c=0.6,0.4$). [As usual, n_c is the electron density value such that ω_{pc}, the plasma frequency corresponding to n_c, is equal to ω_0, the incident (laser) wave frequency.] These values were chosen (i.e., $n_0\geqslant 0.25n_c$) so as to make the usual plasma stimulated Raman scatter (SRS) impossible in order to avoid its complications. Mention was made there of the possible connection with some experimental results at low density ($n_0/n_c\ll 0.25$) by Montgomery *et al.* [2], and analysis by Rose *et al.* [3]. (From here on, the simple ω_p will be used for ω_{p0}, a value corresponding to n_0, the slab peak density.) The experimental results showing a small narrow signal with an uncharacteristic frequency shift of about $0.37\omega_p$ which could not be the usual plasma SRS (also seen but at much higher levels $\sim$3000 times stronger) with its frequency shift of about ω_p. This was interpreted as stimulated narrow-band scattering from long-lived electrostatic excitations at phase velocities comparable to electron thermal velocities and frequencies considerably less than the (relativistic) plasma frequency, a phenomenon which was termed [2] stimulated electron acoustic scattering (SEAS). As has been found in other Vlasov simulations [10] while excitations in this frequency and phase velocity range can be produced if coherently driven up to self-sustaining levels, these excitations are fundamentally nonlinear (they have therefore been termed by those authors KEEN waves for kinetic electrostatic electron nonlinear waves).

On the other hand, it is well known that a one-dimensional, one species (with a fixed homogeneous neutralizing ion background) electron plasma can support spatially inhomogeneous equilibrium structures as shown by Bernstein, Greene, and Kruskal (BGK) [4]. Such an equilibrium is described by a distribution function depending only on the energy of the particle. Using the useful water bag concept [5] and especially when the distribution function is of a two-stream type, the plasma is able to support stationary large amplitude, spatially periodic structures exhibiting "holes" in phase space. The stability of such electron holes has been studied analytically in [6] or numerically in [7]. Periodic electron holes were also studied by H. Schamel [8] and J.P. Holloway and J.J. Dorning [9].

KEEN waves have been studied in periodic Vlasov-Poisson simulations in [10] ponderomotively driven for a short period in time to form self-consistently. By varying the carrier frequency of the drive, it has been found that not only can KEEN waves be sustained nonlinearly and self-consistently (as well as EPW, of course), but that a wide range of frequencies, hitherto thought to be inaccessible for coherent collective wave motion of a plasma (in a band gap between linear electron acoustic waves and EPW) were all legitimately sustainable as well. These studies indicated that this apparent band gap that is indeed there in linear theory, can be filled with highly nonlinear kinetic waves characterized by spatially periodic phase space ″holes″ over a considerable range of velocities.

KEEN waves are quite nonresonant, being relatively easy to drive up over a significant range of frequencies for a given wave number [10]. Now, as remarked before [2], the lack of low-level narrow-band resonance in the electrostatic oscillation precludes the usual stimulated scattering scenario of three-wave resonance amplification from a low-level seed. [In the usual analysis the initial frequency of the scattered electromagnetic wave and the driven electrostatic waves are

chosen to satisfy three-wave resonance. If the electrostatic resonance is very broad the choice of decay wave pairs is hardly constrained at all. The situation resembles the case of highly damped SRS which is in effect stimulated compton scattering (SCS) directly on electrons, ignoring the Langmuir wave "middle man."] How then could something of the SEAS character be produced in the simulations [1] which seem to lack any specific resonance of the longitudinal plasma excitation?

From the work described here, the answer appears to lie in the fact that the simulation plasma was in the form of a relatively sharp-edged slab and this supports (more or less) a previously unrecognized electromagnetic quasimode, a weakly radiating electromagnetic mode structure whose wave vector is determined by the slab width and whose frequency is rather close to ω_p. Because this slab "mode" is not a cavity mode in that the energy can be transmitted through the surrounding medium, it is here termed a radiating plasma slab *pseudomode* or a radiating plasma *pseudocavity mode*. It is the beating of this slab pseudomode with the pump which will define the scattering frequency resonance and the KEEN frequency of about $\omega_0 - \omega_p$. We refer to this unusual plasma slab stimulated scattering process involving the KEEN mode as stimulated KEEN slab scattering (SKSS), to emphasize both requirements, the slab nature of the plasma and the KEEN mode in the plasma. It should be noted that this mechanism can only operate for $n_0/n_c \geqslant 0.25$, and thus does not address the initial excitation difficulty in the SEAS scenario relevant to the low-density experimental results of Montgomery *et al.* [2].

The physics of this radiating plasma cavity mode is likely to be of considerable interest for a wide variety of applications where plasma gradients could be quite steep, such as those related to the Fast Ignitor in laser fusion or high-energy ion acceleration [11] in laser interactions with ultra-thin foils. In particular, a version of SKSS may well be involved in the self-induced transparency (SIT) of an overdense plasma layer.

To obtain our results we used a semi-Lagrangian Vlasov-Maxwell code with only one spatial dimension ($x\omega_p/c$) in the axial wave vector direction [the relevant phase space being ($x\omega_p/c$, p_x/mc)] and the conservation of the canonical momentum for transverse motion. Details of the code may be found in [12]. The semi-Lagrangian Vlasov code displays an extremely low level of numerical noise and proves to be able to describe fine details of accelerated or trapped particles [13] in phase space.

II. NSIS SIMULATION RESULTS

The basic concept of the radiating cavity mode is that, for light waves slightly above the plasma frequency in a plasma slab, i.e., with edges rather thinner than the collisionless skin depth and thickness rather larger than that, there is a very large impedance mismatch of the electromagnetic wave in the plasma with the vacuum, so that this mode radiates only slowly from it from the plasma slab—a pseudo cavity mode rather than a normal cavity mode. It is this radiating *pseudocavity* plasma slab structure that determines the frequency (just above the plasma frequency) and the wave number (some multiple of that, corresponding to twice the slab thickness) of the electromagnetic wave in the plasma which can be combined with the pump frequency and the wave number to produce a well-defined difference ponderomotive force wave drive which can thus drive up the (nonresonant) nonlinear KEEN waves. Because the simulations show that, with a plasma slab and a fairly strong laser field, SKSS may grow much faster than the typical time scale of ion motion, our neglect of ion motion is justified for the simulation used here.

To maintain the connection with the work of Nikolic *et al.* [1], we begin with a similar simulation, a plasma slab of mean density $n_0 = 0.40 n_c$ and an initial temperature of T_e = 20keV. Ions are immobile. The circularly polarized electromagnetic wave is described by a plane wave and is introduced at the left boundary and propagates (in the x direction) through a region of vacuum onto a slab of uniform plasma. The laser amplitude rises approximatively linearly during a time of $150\omega_p^{-1}$, and is then held constant during all the rest of the simulation. The quiver momentum of the electron is $a_0 = 0.30$ (corresponding to an intensity of 0.24×10^{18} W cm^{-2} for a 1 μm wavelength). With λ_{0V} as the incident pump wavelength in the vacuum (with $\omega_0 = (0.4)^{-1/2}\omega_p = 1.581\omega_p$), we consider a uniform plasma of 60 c/ω_p (or $15.1\lambda_{0V}$) length, with a vacuum space of 40 c/ω_p (or $10\lambda_{0V}$) length on both sides. We denote by L_{jump} the small lengths over which the density changes (in a sine-squared profile) from 0 to n_0 and back down again. Here we take $L_{jump} = 10\ c/\omega_p$ (or $2.51\lambda_{0V}$).

The phase space sampling $N_x N_{p_x}$ is 4097×1025, i.e., 4.2 million phase-space cells and the time step $\Delta t\omega_p$ is close to 0.04 (i.e., for a ratio of the space spacing over the Debye length $\Delta x/\lambda_D \simeq 0.045$).

Figure 1 (Color online) gives an example of detailed phase space information available from a Vlasov code such as ours. We focus on the near-final state of the plasma characterized by the formation of a clear KEEN wave. (There is a complicated initial heating process triggered by the pulse arrival and originating at the slab edge transition region which gives considerable rapid heating.) The behavior of the plasma is shown at three different times. Electrostatic trapping structures are clearly visible in the plasma $x - p_x$ phase space, with wave numbers close to k_0 (in the plasma). In Fig. 1 the electron distribution function at $t\omega_p \simeq 337.5$, is shown at the top, showing the end of the sudden acceleration of electrons through early instability with of about 1.1, and the non-Maxwellian distribution function thus produced. This first acceleration instability process "heats" the plasma and creates the conditions (high temperature) required for SKSS to exist. At the next time shown of $t\omega_p \simeq 787.5$, the somewhat shorter wavelength, SKSS KEEN mode has now taken hold at a considerably lower phase momentum $u_\varphi = p_\varphi/mc$ of about 0.55, with the faster electrons from the earlier acceleration riding on top at u_φ of about 1.4. By $t\omega_p \simeq 843.8$ the KEEN mode is beginning to die out somewhat.

Rather than looking at a particular transverse component of electric or magnetic field, it is convenient to solve the Maxwell equations in term of mixed-field combinations associated with propagation to to the right (+) or left (−)

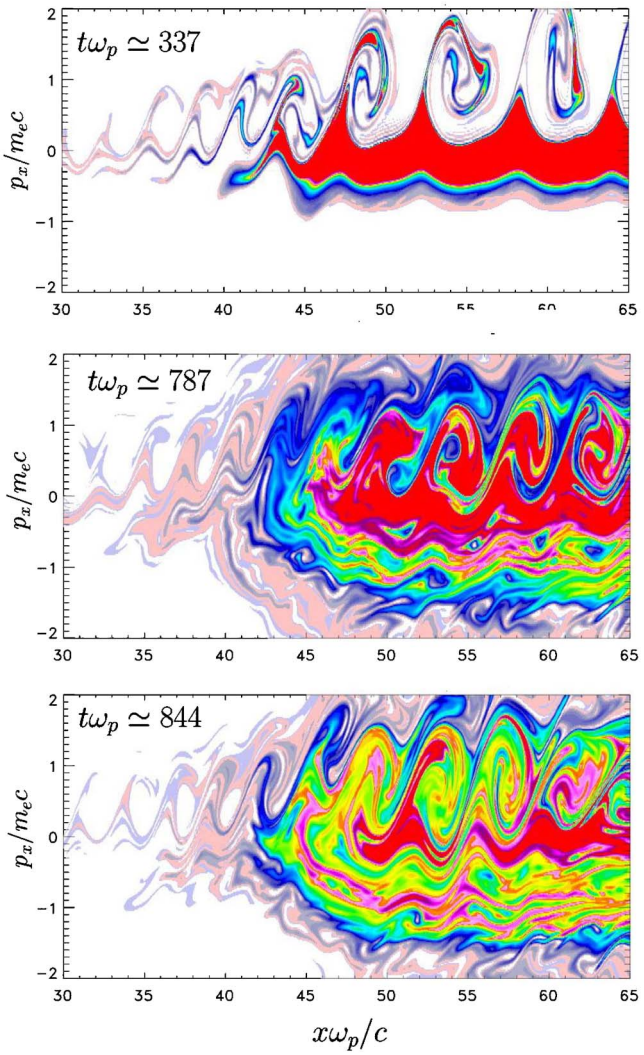

FIG. 1. (Color online) The electron phase space representation afforded by the Vlasov-Maxwell code. The physical parameters are $n_0/n_c=0.4$, $a_0=0.3$ with a laser rise time of $150\omega_p^{-1}$.

directions. The electric and magnetic field components transverse to the x axis are orthogonal and the combined fields are, say, E_{trans} and $\pm\hat{x}\times cB_{trans}$. For instance, in the case of a linearly polarized wave ($E^{\pm}=E_y\pm cB_z$)

$$\frac{\partial E^{\pm}}{\partial t} \pm c\frac{\partial E^{\pm}}{\partial x} = -\frac{J_y}{\epsilon_0}. \tag{1}$$

Hence storing E^+ at the right boundary of the plasma and E^- at the left boundary in vacuum each time step and then time-Fourier analyzing the two resulting arrays, will give, respectively, the backward spectrum (top panel in Fig. 2) and the forward spectrum (middle panel in Fig. 2). The light being circularly polarized we have also introduced the quantities $F^{\pm}=E_z\pm cB_y$. Both spectra have been obtained in the time interval [600–1000] ω_p^{-1} when SKSS is well established.

A three-wave coupling mechanism was observed: a resonant three-wave parametric instability has been observed in simulation involving the incident pump electromagnetic wave (ω_0,k_0), the backscattered electromagnetic wave

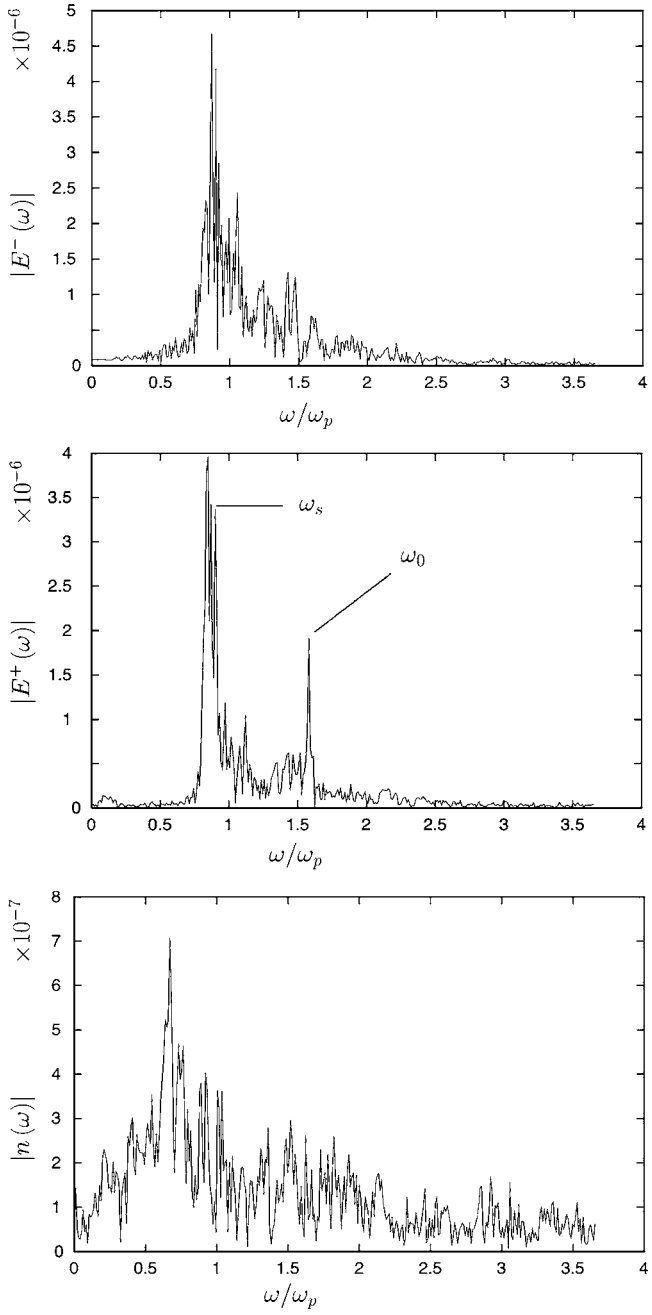

FIG. 2. The electromagnetic backward $E^-(\omega)$ (top panel), forward $E^+(\omega)$ (middle panel) spectra in frequency in NSIT-like simulations with $n_0=0.4n_c$ and $a_0=0.3$.

(ω_s,k_s), and a KEEN wave (ω_K,k_K). The resonant conditions

$$\omega_0=\omega_s+\omega_K \quad \text{and } k_0=-k_s+k_K \tag{2}$$

are well satisfied, while the electromagnetic waves satisfy the standard dispersion relation

$$\omega_{0,s}^2=\omega_p^2\langle\gamma^{-1}\rangle+k_{0,s}^2c^2. \tag{3}$$

We have here $\omega_0=1.581\omega_p$. Estimating the parameter $\langle\gamma^{-1}\rangle$ from the Vlasov simulation (as 0.83), the normalized pump wave number in the plasma from the relativistic dispersion relation is $k_0(\text{plasma})c/\omega_p=1.293$ which is to be

compared with the vacuum value $k_{0V}c/\omega_p=1.581$ given above.

The scattered mode frequency was found to $\omega_s \simeq \omega_p\langle\gamma^{-1}\rangle^{1/2}=0.911\omega_p$ (i.e., $\omega_s/\omega_0=0.58$) in reasonable agreement with the NSIS value [1]. The KEEN wave was observed at the frequency $\omega_K=0.67\omega_p$, i.e., $\omega_K/\omega_0=0.42$ and is still well formed as seen at time $\omega_p t=787.5$ in Fig. 1 with a wave number of $k_K c/\omega_p=1.39$, i.e., $1.08k_0$(plasma). The corresponding phase velocity $v_\varphi=\omega_K/k_K=0.48c$ (which corresponds to $u_\varphi=p_\varphi/mc\simeq 0.55$). More relevant is the comparison with the electron thermal velocity, which began at the 20 keV value of $v_{th}\approx 0.198c$, and increased to $v_{th} \sim u_{th}\langle\gamma^{-1}\rangle c\simeq 0.50c$, $u_{th}=0.60$ and $\langle\gamma^{-1}\rangle\simeq 0.83$ at time $\omega_p t=700$. The KEEN wave phase velocity is about $v_\varphi \simeq 0.96v_{th}$. (Note that the EAW phase velocity is considered to be bounded below by about $1.3v_{th}$ [3], that was for a nonrelativistic plasma.) At $\omega_p t=843.8$ in Fig. 1 the wave structure is deteriorating (probably because the returning phase-mixed electrons are difficult to trap cleanly), the heating of the electrons has ceased, and the scattered wave power has dropped significantly. The plasma has apparently now become too hot to support a KEEN wave of the resonance phase velocity. This effect was also observed in the electromagnetic spectra which exhibits a weak shift in frequency till $\omega_s=0.85\omega_p$ (leading to $\langle\gamma^{-1}\rangle=0.73$) presumably due to the increase of the temperature during the evolution. So far we have essentially confirmed the NSIS results with no new physics.

III. SKSS IN A HOT PLASMA

The main difficulty in resolving SKSS from the standard SRS in laser-plasma experiments with the maximum plasma frequency less than the laser frequency is that the density variation is usually very gradual. (Sharp-edged plasmas have densities far above critical density; letting the plasma spread makes the density transition very broad.) For central plasma densities below the critical density and above the quarter-critical density (and thus favorable for KEEN phenomena) the initial rapid development of SRS in the lower density corona complicates the situation considerably. The situation is more favorable in an initially hot plasma where the growth rates of SRS are significantly reduced, allowing SKSS to be the dominant mechanism.

Our simulation parameters were chosen in the following way. In order to concentrate on the KEEN wave aspects rather than the initial complicated electron heating process, we have increased the initial plasma temperature to $T_e=400$ keV, so that (a) the initial complications were suppressed by the high Landau damping of any SRS-like processes, and (b) the KEEN process itself did not have to wait for its fast electrons to be produced by heating from some other mechanism. We also took the mean electron density to be somewhat higher, namely $n_0=0.6n_c$, to correspond to the other NSIS value [1]. The quiver momentum of the electron is $a_0=0.5$, corresponding to 0.68×10^{18} W cm^{-2} and the laser rise time is 750 ω_p^{-1}. In this example the plasma is initially only $60c/\omega_p$ long, with a vacuum space of $40c/\omega_p$ long on both sides. The value was kept the same for the plasma edges, namely, $L_{jump}=10c/\omega_p$.

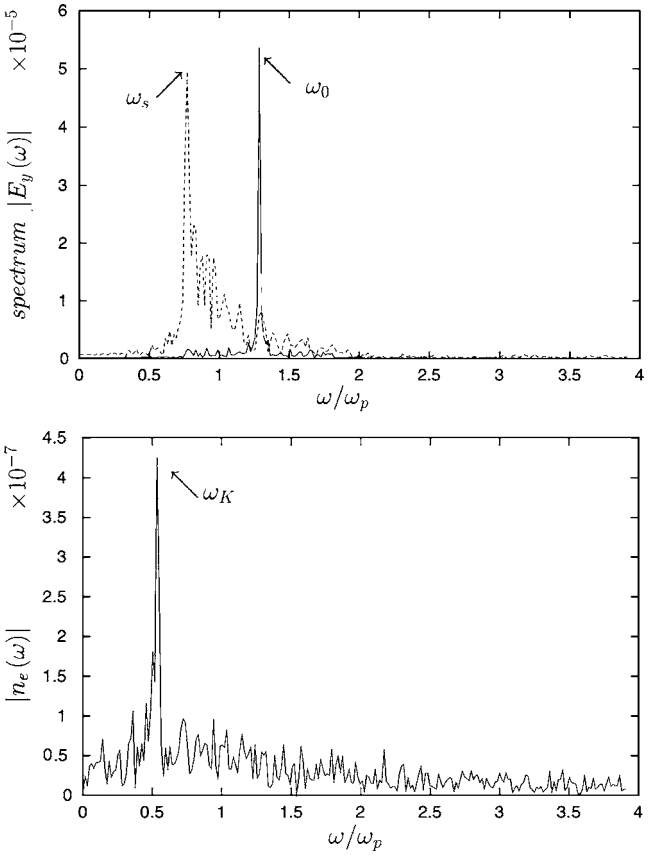

FIG. 3. Backward (shown 20 times larger in dashed line in the top panel) and forward (shown in solid line) electromagnetic spectra obtained when the instability is well established. The physical parameters are $n_0/n_c=0.6$, $a_0=0.5$.

The forward spectrum of Fig. 3 exhibits clearly the peak at the pump frequency $\omega_0=1.290\omega_p$ (in agreement with the predicted value of $(n_0/n_c)^{1/2}$ close to 1.29099). The corresponding wave number k_0 was estimated close to $k_0c/\omega_p=1.032$. Previous values ω_0 and k_0 indeed satisfy the standard dispersion relation (3) using $\langle\gamma^{-1}\rangle\simeq 0.60$, estimated directly in Vlasov simulation. Figure 3 indicates the existence of a backscattered wave at ω_s which is again found (upper frame of Fig. 3) to be driven near critical, i.e., $\omega_s \simeq \omega_p\sqrt{\langle\gamma^{-1}\rangle}\simeq 0.77\omega_p$ which again implies $k_s\simeq 0$. The resonant conditions (2) are again well satisfied in this simulation as shown in the lower panel of Fig. 3, showing the spectrum of the electron density (at $x\omega_p/c=90$) which clearly exhibits a peak at the expected difference KEEN frequency $\omega_K=0.52\omega_p$ (well below the plasma frequency including the relativistic and temperature effects $\omega_p\sqrt{\langle\gamma^{-1}\rangle}$). Analysis of the spectrum in k (not shown here) gives as it should $k_K \simeq k_0$. The apparent backscattered Stokes mode is really half the loss from the radiating cavity mode.

The physical parameters for the code run of Fig. 4 showing the electron phase space are unchanged from those of Fig. 3, except that now the laser rise time is taken here to be $450\omega_p^{-1}$. Figure 4 is color online. We see clearly nine or ten vortices for a plasma length of $9.85\lambda_0$ indicating that the

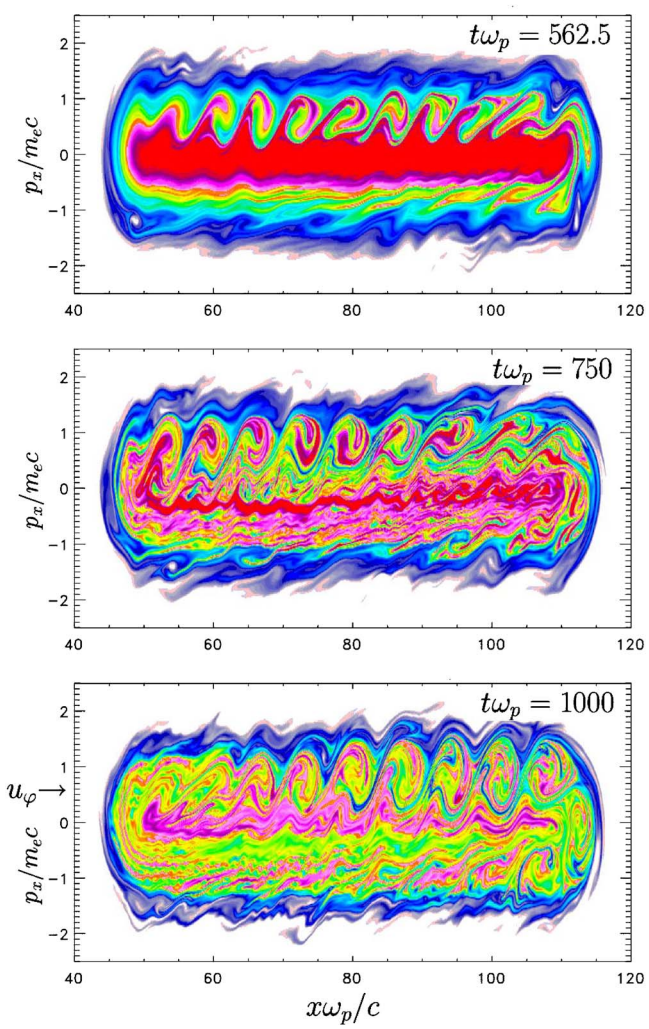

FIG. 4. (Color online) The electron phase space representation showing the formation of (nine) trapping structures in a $9.4\lambda_0$ plasma length. The physical parameters are $n_0/n_c=0.6$, $a_0=0.5$ with a laser rise time of $450\omega_p^{-1}$.

longitudinal wave number k_K (as revealed by the trapped electron phase space vortices) is close to the k_0 value in the plasma. As the instability evolves to a mixed electrostatic/electromagnetic regime, the trapping structures seen in phase space represent a nonsteady variant of the well-known BGK modes that describe invariant traveling electrostatic waves in plasmas. As shown in the earlier phase space frame ($\omega_p t=562.5$) of Fig. 4, the SKSS for this hot plasma has now developed in a much cleaner fashion than for the case of low initial temperature (compare with Fig. 1), showing strong clean trapping effects for less intense electrostatic fields. (For negative values of momentum one sees the electron recirculation from the right-hand plasma edge, with clear phase mixing convection as the electrons return upstream against the propagating KEEN wave.) By the later frame ($\omega_p t=1000$) of Fig. 4 the KEEN wave is beginning to break up. In the example of Fig. 4, the backscattered electromagnetic wave here in the plasma is actually a radiating plasma cavity mode with a wavelength (rather than a half wavelength) equal to the plasma slab thickness. The longitudinal plasma

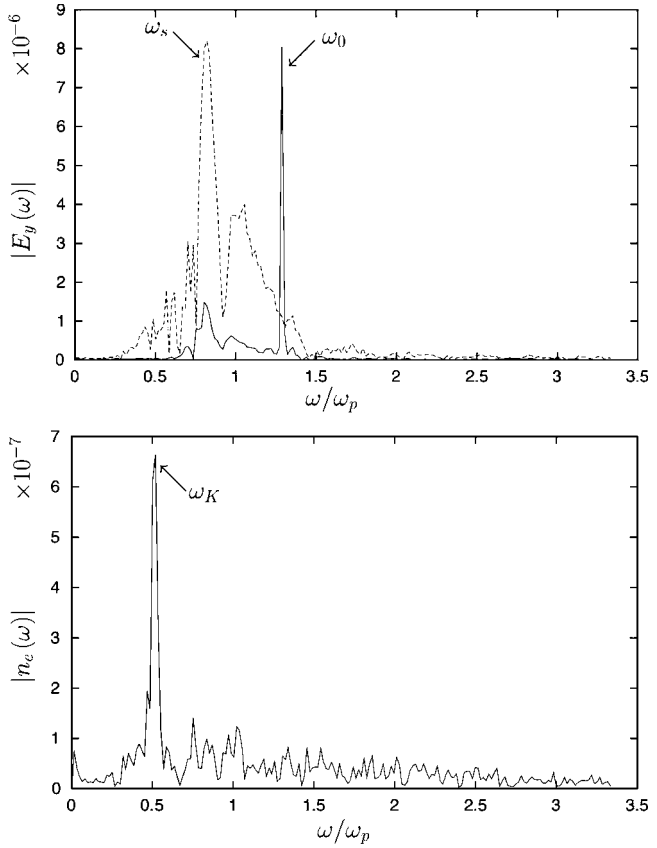

FIG. 5. The electromagnetic spectra (top panel, backward in dashed line) and electrostatic spectrum (bottom panel). The physical parameters are $n_0/n_c=0.6$, $a_0=0.5$.

excitations thus produced in Fig. 4 have phase velocity $v_\varphi=\omega_K/k_K$ close to 0.50c (which corresponds to $u_\varphi=p_\varphi/mc=0.577$). This is in fact now considerably less than the electron thermal momentum (which, for 400 keV, is $u_{th}=p_{th}/mc=0.884$). This is quite unlike EAW phase velocities, which (as mentioned above) are considered to be bounded from below by about $1.3v_{th}$ [3]. Because the phase velocity is far below the lowest value in the EAW presentations [3], the electron-kinetic waves are not EAW in nature and are thus definitively KEEN waves for which a much wider range of frequencies is possible [10].

Let us now discuss whether allowing movement of the ions with realistic charge to mass ratios will significantly alter SKSS. It is well known that fixed ions act to prevent the electron expansion. The effect of mobile ions is to modify somewhat the plasma edges over several pump wavelengths, but without changing significantly the structure of the ambipolar field which affects the sheath through which the KEEN excitations are reflected. This test simulation was carried out using $\tau\omega_p=450$, $a_0=0.50$ and $n_0/n_c=0.60$. The ratio of the ion mass to the electron mass is $M/m=1836$ (appropriate to protons) and we take an initial ion temperature of $T_i=25$ keV (high enough to observe possible ion effects) the electron initial temperature being $T_e=400$ keV.

As one might expect, the addition of realistic ions has little effect. This can be seen from the electromagnetic spectra given in Fig. 5 (top panel), not to mention the electro-

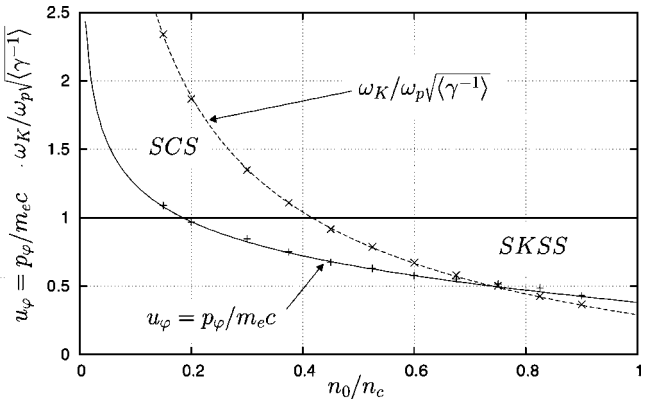

FIG. 6. A display of the normalized plasma phase momentum $u_\varphi=\gamma_\varphi\beta_\varphi$ where $\beta_\varphi=\omega_K/k_K c$ and og the frequency ratio of the KEEN waves to the relativistic frequency as a function of n_0/n_c. Crosses are determined via numerical Vlasov simulations at a given value of n_0/n_c.

static spectrum in the bottom panel measured in the range $[350\omega_p^{-1}-700\omega_p^{-1}]$. The electromagnetic spectrum with mobile ions shows no significant change when compared with the spectrum of Fig. 3 with immobile ions. The forward spectrum (plotted here in a solid line in top panel) gives a pump frequency close to $\omega_0=1.290\omega_p$ while the backward spectrum (plotted $2\times$ larger, in dashes) is wide with a dominant peak at $\omega_s\simeq 0.78\omega_p$ (here $\langle\gamma^{-1}\rangle\simeq 0.62$) and $\omega_p\langle\gamma^{-1}\rangle^{1/2}\simeq 0.787\omega_p$. The analysis of the density spectrum leads to a KEEN frequency of $\omega_K=0.51\omega_p$, close to the expected value of the beatwave $\omega_0-\omega_s=0.51\omega_p$.

For mobile ions we found that not only can KEEN waves be sustained nonlinearly and self-consistently but also that SKSS can persist for somewhat more gradual plasma edges, but still keeping fairly sharp plasma edges, a condition required for strong radiating plasma cavity.

IV. PRODUCTION OF SKSS IN HOT PLASMA FOR A WIDE RANGE OF DENSITIES

We focus now on the production of SKSS for a range of plasma densities and the same plasma thickness. Several simulations were carried out in the case of a homogeneous and hot (400 keV) plasma with a thermal $\langle\gamma^{-1}\rangle^{1/2}$ value of about 0.77 to confirm the existence of SKSS and the generation of low-frequency KEEN waves for a wide range of value of n_0/n_c. In these simulations, n_0/n_c was varied from 0.15 to 0.975. As can be seen in Fig. 6, which displays the normalized plasma phase momentum u_φ and the frequency ratio of the KEEN wave to the relativistic plasma frequency $\omega_K/\omega_p\langle\gamma^{-1}\rangle^{1/2}$ as a function of the ratio n_0/n_c, it is possible to excite a KEEN wave over a wide range of phase velocities and frequencies. The solid lines were obtained by estimating u_φ and ω_K directly from the SKSS scenario, using the matching conditions in frequencies and wave numbers of Eqs. (2). (We have then determined the quantity $u_\varphi=v_\varphi\gamma_\varphi/c$ by taking $v_\varphi=\omega_K/k_K\simeq[\omega_0-\omega_p\langle\gamma^{-1}\rangle^{1/2}]/k_0$ where $\gamma_\varphi=1/\sqrt{1-\beta_\varphi^2}$ and $\beta_\varphi=v_\varphi/c$.) The numerical estimation values obtained from the actual Vlasov simulations are represented by crosses on the curve. These values were measured by analyzing the spectra in frequency and wave vector of the electromagnetic and plasma fields. The system length used here was taken as $L_{slab}\omega_p/c=60$ and the laser rise time is $\tau\omega_p=450$.

The close agreement between the curves and the simulation results clearly shows that the initial NSIS observation [1] that the scattered frequency is very close to the relativistic plasma frequency applies for a very broad range of normalized plasma densities n_0/n_c, i.e., from 0.15 to 0.9. At these high temperatures it is also clear that one can say that (roughly) for n_0/n_c values from 0.4 to 0.9, one is scattering from KEEN waves (whose frequencies are below the relativistic plasma frequency), while for n_0/n_c values from 0.15 to 0.4 one is scattering from (highly damped) Langmuir waves whose frequencies are above the relativistic plasma frequency. However, it is equally valid for these hot plasmas to regard all these scattering results as stimulated Compton scattering (SCS) from electrons over the whole range of n_0/n_c from 0.15 to 0.9, with little part being played by the conventional weakly damped electrostatic plasma waves.

To further investigate the possibilities of coupling, we present now in detail the result of a simulation which was performed with $n_0/n_c=0.30$ (and $a_0=0.50$) just above the usual nonrelativistic limiting quarter-critical density value. Spectra of the forward $(eE^+/m\omega_p c)$ and backward $(eE^-/m\omega_p c)$ propagating electromagnetic fields, respectively, are shown in the top and middle panels of Fig. 7. The bottom panel corresponds to the electrostatic spectrum (here the spectrum of the electron density). The top panel exhibits clearly two main transmission peaks: the first one corresponds to the scattered light at frequency $\omega_s\simeq 0.78\omega_p$ which corresponds to the (relativistic) plasma frequency $\omega_p\langle\gamma^{-1}\rangle^{1/2}\simeq 0.78\omega_p$ (we have used here from Vlasov data $\langle\gamma^{-1}\rangle\simeq 0.60$). The second peak is the expected pump frequency at $\omega_0=1.8257\omega_p$. The middle panel of the back-emitted radiation shows a more complex spectrum, with, however, a dominant peak at frequency $\omega_s=0.770\omega_p$ which characterizes the radiation from the pseudocavity mode. (Recall that the radiating plasma cavity radiates in both directions.) In the bottom panel the signature of the KEEN wave is clearly visible at frequency $\omega_K=1.045\omega_p$. (The Bohm-Gross relation will give an estimation of the EPW frequency as $\omega_{EPW}=(\omega_p^2\langle\gamma^{-1}\rangle+3k_K^2v_{th}^2)^{1/2}\simeq 2.10\omega_p$ (using here $v_{th}/c=u_{th}\langle\gamma^{-1}\rangle=1.20\times 0.61=0.73$). Note that at such a hot temperature, EPW will be severely Landau damped since we have $k_K\lambda_D=1.2$.

Thus the pump wave scatters from KEEN waves according to the expected matching conditions ($\omega_0=\omega_s+\omega_K$ and $k_0=\pm k_s+k_K\simeq k_K$). Here $k_0(\text{plasma})c/\omega_p\simeq 1.65$ (which is to be compared with $k_{0V}c/\omega_p\simeq 1.825$) which gives using the dispersion relation for circularly polarized wave $(\omega_p^2\langle\gamma^{-1}\rangle+k_0^2c^2)^{1/2}\simeq 1.82551\omega_p$ and which is good agreement with the numerical value observed in the electromagnetic spectra. The corresponding wave vector is $k_K\simeq 1.55\omega_p/c$.

Figure 8 displays the electron distribution function in phase space corresponding to Fig. 7, showing the SKSS characteristically strongly nonlinear trapped particle modes. We found that strong trapping effects occur for even small-amplitude electrostatic waves, resulting in undamped travel-

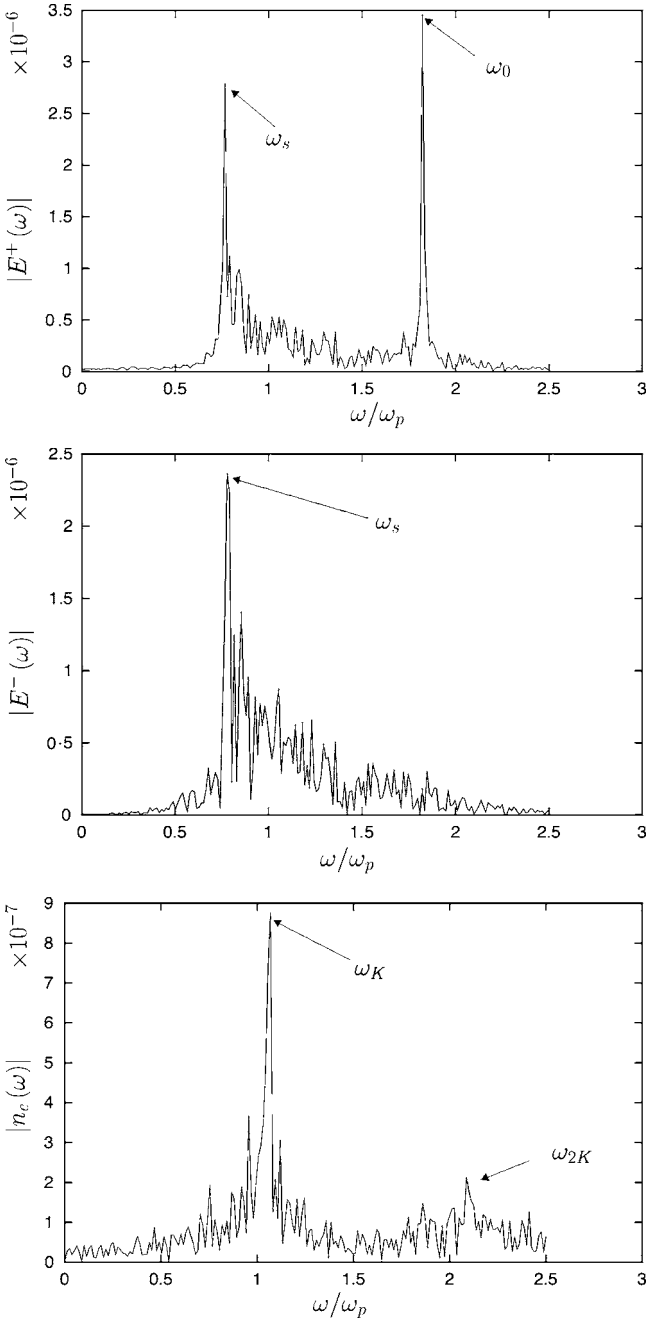

FIG. 7. Frequency spectra in the case of a Vlasov simulation using $n_0/n_c=0.30$ and $a_0=0.5$: forward spectrum in the top panel, backward spectrum in the middle panel, and electrostatic spectrum (electron density) in the bottom panel.

ing waves. Approaching the right boundary, positive mean velocity trapping vortices "orbit" clockwise in phase space at the right-hand boundary and then move left along the momentum coordinate at about $u_\varphi=-1.4$, but with clear evidence of disruption as they penetrate the excitation region of the rightward-driven SKSS.

The lack of low-level narrow-band resonance for KEEN waves of negative velocities means that these modes essentially disappear by phase mixing when they are reflected. The phase space velocity is then easily and accurately measured as $v_\varphi \simeq \omega_K/k_0=1.802/2.463$ or $v_\varphi \simeq 0.731c$ (i.e., $u_\varphi=0.90$).

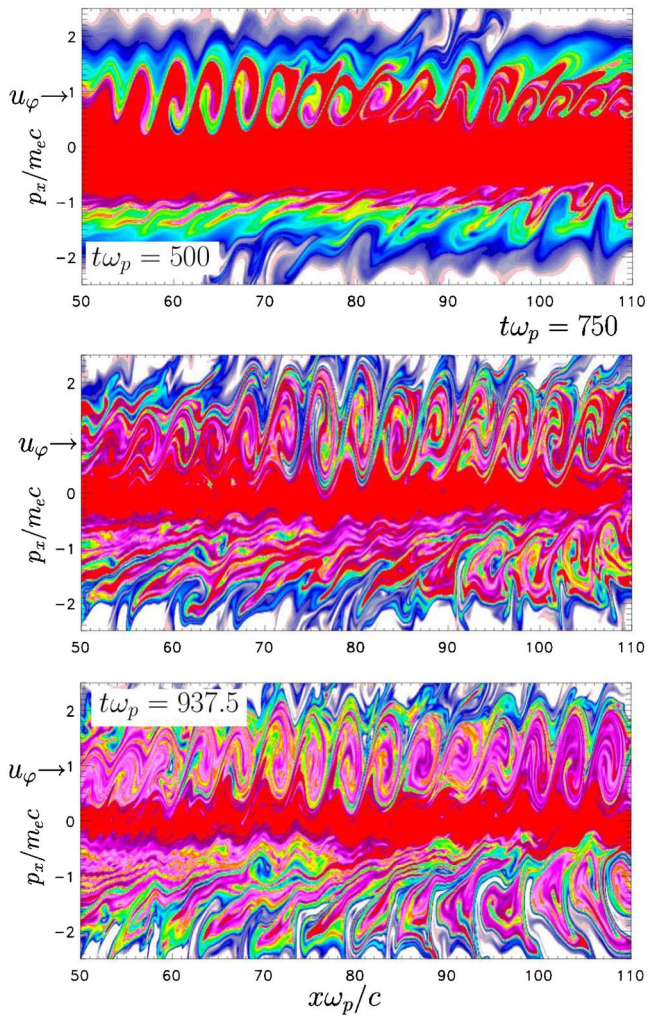

FIG. 8. (Color online) A display of the electron distribution function in phase space. The physical parameters are $n_0=0.30n_c$ and $a_0=0.50$. We see clearly the formation of trapping structures. The lack of low-level narrow-band resonance for KEEN waves (of negative velocities) shows that these modes are destroyed when they are reflected.

This value is above the thermal velocity and close to $p_\varphi \simeq 0.750p_{th}$ (where $v_{th}/c=u_{th}\langle\gamma^{-1}\rangle \simeq 1.200\times 0.61=0.73$), which is close here of the dispersion relation of trapped electron acoustic waves.

V. RADIATING PLASMA PSEUDOCAVITY: THE EFFECT OF MORE GRADUAL PLASMA EDGES

In order to test our contention that fairly sharp boundaries are vital to setting the scattered electromagnetic wave frequency close to the plasma frequency, we have also investigated plasma-edge densities which change spatially rather more gradually than those investigated so far. While a simple theory exists for sharp plasma boundaries, for somewhat slower density variation at the edges, we must resort to simulations (in which the laser field is kept sufficiently low so that SKSS does not dominate). Clearly a profile should be used which reflects the normal expansion of a plasma before

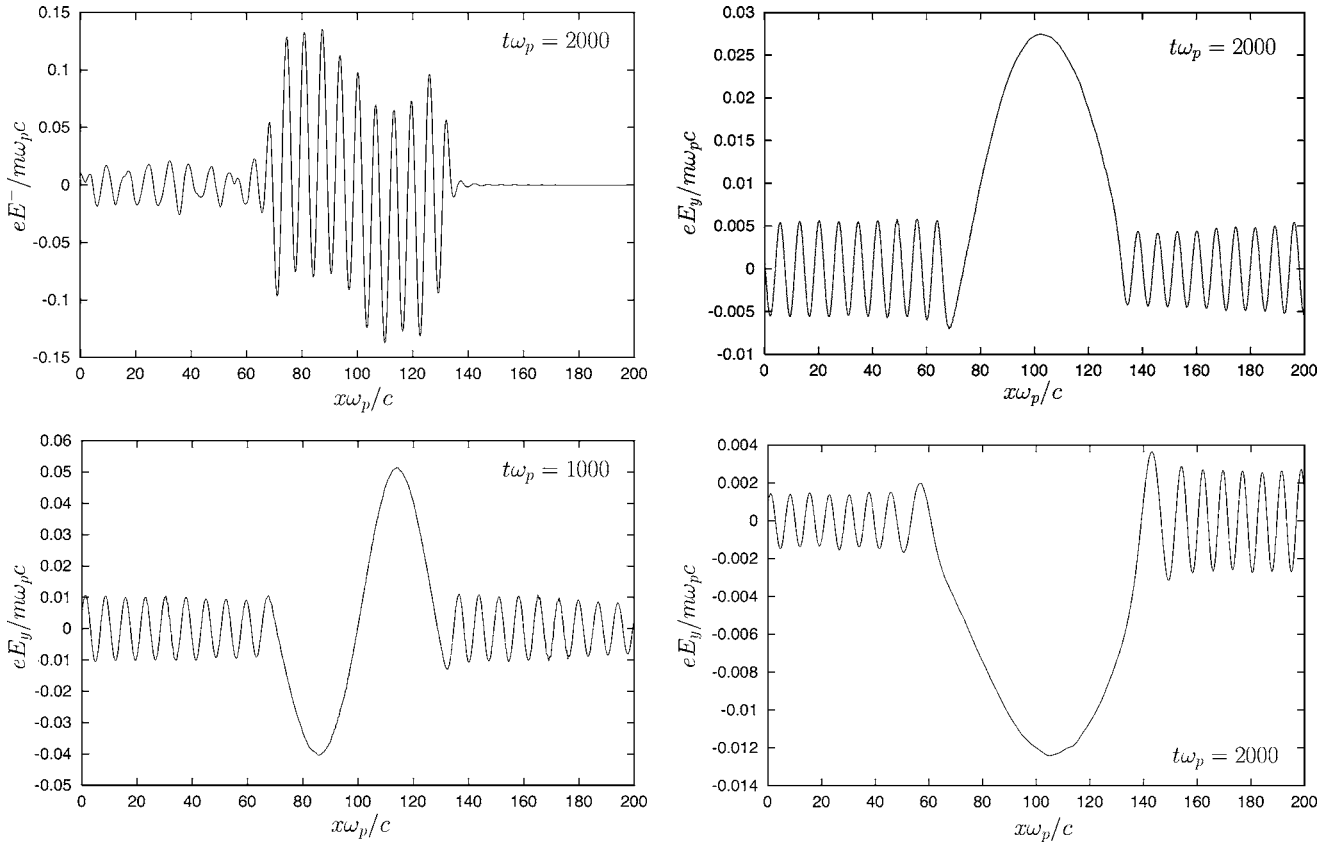

FIG. 9. The $E_y - cB_z$ contribution of the electromagnetic field (top left panel), the cavity is driven in full-wavelength resonance. By implementing the radiating plasma slab cavity as an initial condition with full wavelength for the electromagnetic field, it was found that the cavity is stable till time $t\omega_p = 1000$ (bottom left panel) but the asymptotic state (top right panel) at time $t\omega_p = 2000$ shows a dominant mode on half wavelength. Another simulation was performed with more gradual plasma edges, which indicates that the system has evolved, leading to modification of the length of the plasma slab cavity.

the arrival of the laser beam, rather than some arbitrary choice. Rather than wait for a plasma slab with moving ions to spread thermally (not to mention the complication of changing ambipolar potential), it proved more convenient to explore this aspect of the effect of more gradual edges, by setting up such profiles at the outset using fixed ions for convenience. We start first with a Vlasov simulation which takes into account the propagation of the pump wave allowing the formation of the plasma radiating slab mode in a self-consistent way. As before we chose $n_0/n_c = 0.60$ and $T_e = 400$ keV. The plasma slab cavity is located between $70c/\omega_p$ and $130c/\omega_p$ and is kept fixed in the different simulations which have been carried out.

First we considered a plasma slab with fairly sharp edges, i.e., with $L_{jump} = 6c/\omega_p$ corresponding to a strong cavity effect. We also took $a_0 = 0.30$, i.e., a value just above the pump laser threshold required to start up the instability which was numerically estimated to be close to $a_{0thres} \simeq 0.20$. From the ratio of the electron density to the critical density ($n_0/n_c = 0.60$) we deduce the exact value of the pump frequency at $\omega_0 \simeq 1.291\omega_p$. The analysis of electromagnetic spectra (not shown here) leads to a scattered light with a frequency of $\omega_s = 0.840\omega_p$ and the corresponding KEEN wave is observed at frequency $\omega_K = \omega_0 - \omega_s \simeq 0.45\omega_p$. With $\langle \gamma^{-1} \rangle \simeq 0.70$ [which corresponds here to a (relativistic) plasma frequency $\omega_p \langle \gamma^{-1} \rangle^{1/2} \simeq 0.836\omega_p$] we find the value of the pump frequency from the linear dispersion relation to be close to $\omega_0 = (\omega_p^2 \langle \gamma^{-1} \rangle + k_0^2 c^2)^{1/2} \simeq 1.288\omega_p$ using a value of the pump wave vector in plasma of $k_0 c/\omega_p = 0.98$.

Insight into the plasma slab cavity formation can be gained by considering the $E^- = E_y - cB_z$ contribution of the electromagnetic field inside the plasma (note that outside the plasma this field describes the backward propagating part of the electromagnetic field in vacuum). This quantity is plotted in the top left panel of Fig. 9 as a function of $x\omega_p/c$ at time $t\omega_p = 2000$, i.e., in the asymptotic state. Inside the slab the combination is seen to consist of the pump (at the normalized wave number 0.98) and the scattered mode at ω_s which clearly has one full wavelength in the cavity, with $k_s c/\omega_p = 2\pi c/\omega_p L_{slab} \simeq 0.104$ and thus $\omega_s = (\omega_p^2 \langle \gamma^{-1} \rangle + k_s^2 c^2)^{1/2} \simeq 0.843\omega_p$. Thus the wave vector of this weakly radiating mode is directly determined by the slab width and a frequency close to the (relativistic) plasma frequency.

It is not yet clear to us why the mode "selected" by the system is not the expected "ground state" with a wave number of half that value seen. To address this point, the cavity mode evolution was studied by turning off the laser pulse and implementing directly the radiating plasma slab cavity as an initial condition with a full wavelength in the electromagnetic field in the code. (We chose here $a_0 = 0.20$. Note also

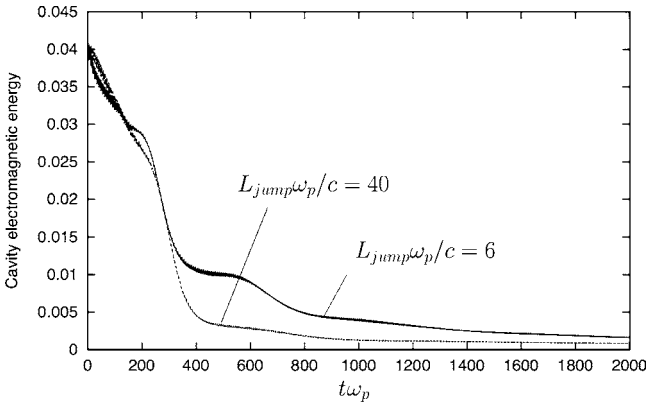

FIG. 10. The electromagnetic energy W_0 of the plasma slab cavity: the solid line corresponds to $L_{jump}\omega_p/c=6$, while the dotted line is related to the case where $L_{jump}\omega_p/c=40$. The depletion of the energy is, however, more rapid in the case where the slab boundaries are made sufficiently gradual.

the radiated field outside the pseudocavity.) The modified profile mode was indeed observed to then evolve towards the expected characteristic "ground" state of half-wavelength, as shown in the upper right panel of Fig. 9 at time $t\omega_p=2000$. At $t\omega_p=1000$ the full-wavelength state is still present as shown in the left bottom panel, but by $t\omega_p=2000$ the asymptotic state in the upper right panel of Fig. 9 indeed shows the expected mode at one half-wavelength. The mystery still remains as to why the plasma "prefers" the full wavelength mode at earlier times. The likely reason is additional coupling between pump and scattered wave at the plasma edges.

Another simulation was now performed with more gradual plasma edges with $L_{jump}\omega_p/c=40$. A result for that case is presented in the bottom right panel of Fig. 9. One sees which indicates that the system has evolved again towards the ground state, i.e., towards a cavity of larger length (but now more weakly inhomogeneous).

The second point which emerges from these numerical simulations is the fact that the radiating plasma cavity mode is continually sustained by the injected pump wave (when taken into account in full-Vlasov simulations). In effect this coupling prevents the cavity from reaching its ground state and losing all its energy. The plasma slab constitutes thus a fairly high Q-cavity for electromagnetic waves over a long time.

We obtained an estimate of the pseudocavity quality factor Q in the initial phase of the instability (i.e., for $t\omega_p \leqslant 500$) by computing the total electromagnetic energy W_0 of this plasma slab cavity as $W_0=\int_{L_{slab}} w_{em}(x,t)dx$ where the electromagnetic energy density was taken as

$$w_{em} = \frac{\mu_0}{4}|\mathbf{H}|^2 + \frac{\epsilon_0}{4}\mathbf{E}^* \frac{\partial}{\partial \omega}(\varepsilon_r \omega)\mathbf{E}. \tag{4}$$

Here ε_r is the transverse relative dimensionless dielectric coefficient and ε_0, μ_0 are the usual SI vacuum quantities, while E and B are the appropriate electric and magnetic fields. Numerical results are shown in Fig. 10. The solid line corresponds to $L_{jump}\omega_p/c \simeq 6$ while the dotted line is related to the case of more gradual plasma edges where $L_{jump}\omega_p/c \simeq 40$. Using the relation

$$Q^{-1} = \frac{1}{\omega_s}\frac{\partial \ln W_0(t)}{\partial \omega} \tag{5}$$

we obtain $Q \simeq 430$, while an analytical prediction based upon the formula

$$Q^{-1} = 2\pi\left(\frac{c}{L_{slab}\omega_p}\right)^2\left(\frac{\omega_p}{\omega_0}\right)^2 \tag{6}$$

gives $Q \simeq 424$, in good agreement with the previous numerical result. The depletion of the energy is, however, more rapid in the case where the slab boundaries are made sufficiently gradual, but it is not easy to give an analytic answer for this case. Figure 10 indicates, at time $t\omega_p=500$ that typical losses are close to 90% for more gradual plasma edges (with $L_{jump}\omega_p/c \simeq 40$) and 75% for sharp edges (with $L_{jump}\omega_p/c \simeq 6$).

VI. RADIATING PLASMA PSEUDOCAVITY: THE EFFECTS OF PLASMA SLAB WIDTH

The results just discussed shed light on the existence of this radiating plasma cavity and the importance of sharp plasma edges. We focus now on the effects induced by changing the width of the plasma slab on the SKSS instability. As previously mentioned, this instability appears in the form of a (three-wave) parametric instability in which the candidate waves must match the three-wave resonance conditions (2). However it is nearly always possible to drive simultaneously the transverse mode $(\omega_s, \pm k_s)$ through backward or forward scattering. In fact the cavity radiates in both directions. At a given time one of the processes (backward or forward scattering) is predominant in simulation.

First, for these driven waves the range of frequencies over which these trapped-electron modes can be driven at a given wave number is very broad and is in fact not determined by the amplitude of the electrostatic potential. Therefore, for a three-wave scattering instability with a given pump, if the kinetic wave can be driven over a very broad frequency range for a given k_K, then its resonance will not determine the three-wave resonance, but something else will determine the resonance. In fact it is an electromagnetic daughter wave that sets the resonance via a cavity mode. For sharp-edged plasmas with nearly uniform density inside the edges, all electromagnetic modes are not equally favored as in the infinite uniform system. In the case of the plasma slab, the electromagnetic modes with an integer number of half wavelengths in the plasma slab are favored at earlier times, and the lowest modes have most of all.

The SKSS instability wave number thus depends on the plasma slab width. In order to address this point, we perform a set of numerical simulations in which we let the slab width L_{slab} vary. We use physical parameters identical to those previously used in Fig. 3 and in Fig. 4, namely $n_0/n_c=0.60$ and

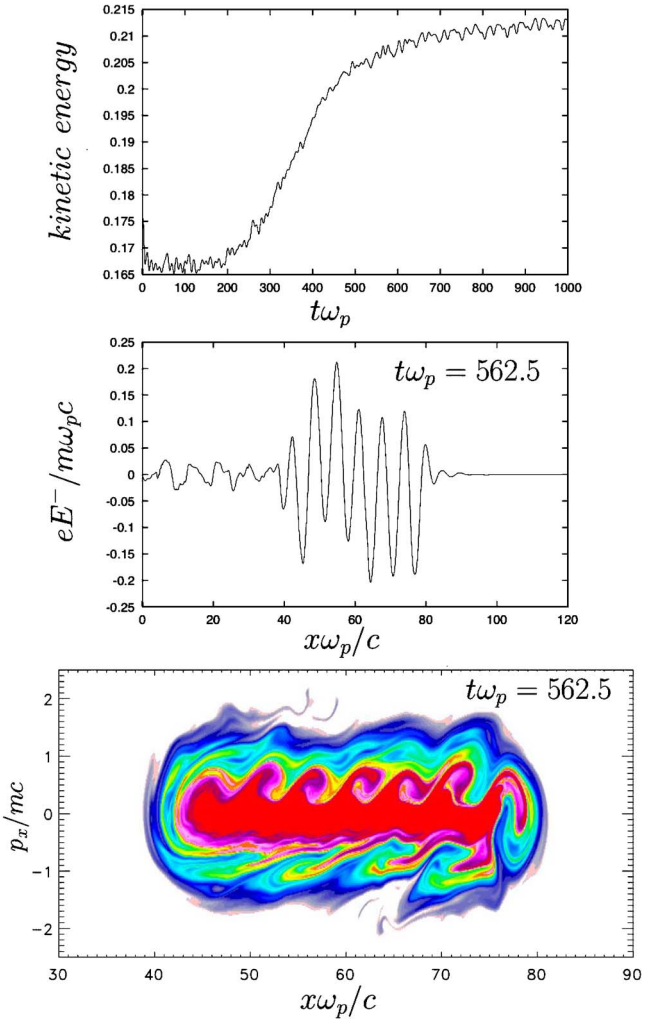

FIG. 11. (Color online) The numerical results obtained in the case of a plasma slab length L_{slab} of $30c/\omega_p$: relativistic kinetic energy versus time (top panel), $eE^-/m\omega_p c$ contribution of the electromagnetic field versus space $x\omega_p/c$ at time $t\omega_p=562.5$, showing wavelength modulation of the envelope (middle panel) and finally phase space behavior showing KEEN wave at the same time (bottom panel and color online). Physical parameters are $n_0=0.6n_c$, $a_0=0.5$, and $T_e=400$ keV. Ions are kept fixed.

$a_0=0.5$. Since the observation of KEEN waves is greatly facilitated in a hot plasma, we keep $T_e=400$ keV for the electron plasma temperature. Different values of the slab width L_{slab} were used in the simulations (keeping, in each simulation, the same numerical resolution in time and in phase space). The time step was chosen to $\Delta t\omega_p \simeq 0.039$ and and the elementary phase space cell is given by $\Delta p_x/mc \simeq 0.020$ and $\Delta x\omega_p/c \simeq 0.039$. For example, Fig. 11 shows simulation results obtained in the particular case of the plasma slab length L_{slab} of $30c/\omega_p$. (In each case the plasma slab was surrounded by the same vacuum region of $40c/\omega_p$ on both sides and the jump which characterizes the vacuum-plasma interface is $L_{jump}=10c/\omega_p$.)

Figure 11 shows in the top panel the time evolution of the mean (relativistic) kinetic energy given by

$$\frac{K}{mc^2} = \int_0^L \frac{dx}{L} \int_{-\infty}^{+\infty} dp_x(\gamma - 1) f(x, p_x, t) \tag{7}$$

(L being the total system length) which gives a history of the entire simulation. The radiating plasma cavity formation is accompanied by modest ($\sim 15\%$) increase of the total kinetic energy followed by an asymptotic phase in which KEEN waves stay in resonance for relatively long periods. This time-varying diagnostic in kinetic energy allows us to find when the radiating plasma cavity is forming and to estimate the beginning of the asymptotic regime, since the time evolution depends on the size of the plasma. An indication concerning the creation of this radiating plasma cavity is then given in the middle plot in Fig. 11 at time $t\omega_p=562.5$. We have plotted the $eE^-/m\omega_p c$ contribution of the electromagnetic field versus space $x\omega_p/c$ (here E^- denotes the quantity $E_y - cB_z$). Although the cavity radiates in both directions, the analysis of the cavity formation is simplified by considering this diagnostic even when the forward scattering predominates in plasma. The reason is the fact that E^- provides precise information on the cavity amplification by eliminating almost all of the pump contribution. (The elimination is not total because there is some normal backscattering from the plasma edges.) The usual spectrum diagnostic in k does not allow us to determine k_s very well, since k_s is here of the same order as the precision level afforded by a Fourier analysis. The $eE^-/m\omega_p c$ result shows two phenomena: a fast oscillatory structure within the cavity region (the pump backscatter) plus a single spatial cycle ($2\pi/L_{slab}$, which is here close to $0.20c/\omega_p$) in the plasma due to the scattered wave close to the plasma frequency.

The last image (bottom panel and color online) shows the corresponding phase space behavior at the same time. From the distribution function, we have estimated the corresponding wave vector k_K of the KEEN wave close to $k_K c/\omega_p \simeq 1.25$ (the cavity region presents indeed six holes, i.e., 6 wavelengths; the wavelength of the KEEN wave is thus close to $\lambda_K \simeq L_{slab}/6 = 5.45c/\omega_p$ or equivalently $k_K c/\omega_p \simeq 1.25$). Using $\langle \gamma^{-1} \rangle \simeq 0.615$ and the dispersion relation (3), the pump wave frequency is then close to the value $\omega_0 \simeq 1.2905\omega_p$. At time $t\omega_p=562.5$ the matching conditions in wave vectors gives $k_0=-k_s+k_K$ ($1.025=-0.23+1.255$ in ω_p/c units). The corresponding matching conditions in frequencies is $\omega_0=\omega_s+\omega_K$ ($1.290=0.79+0.50$ in ω_p units).

We have examined this kind of behavior for two longer slabs with lengths, namely L_{slab} of $60c/\omega_p$ and L_{slab} of $100c/\omega_p$. The data for each case look generally very similar to that of Fig. 11 (so for brevity we do not present them here), and verify the basic proposition that the electromagnetic scattered mode has only a few half cycles in the slab. This means that the scattered light wave number is far below the characteristic wave number ω_p/c and so its frequency is very close to the (relativistic) plasma frequency, thus the basic concept has been thoroughly tested. In each of these cases we have also verified (in the same way as for the case just discussed) that the three-wave frequency and wave-number resonance relations are respected in detail.

There is, however, a slight modification to the original picture, in which the concept was that the scattered wave

number would likely be in the lowest wave-number or ground-state mode. It appears that for the larger slabs it is more likely that the initial scattered light wave number begins at a value which, while low (a small number of half wavelengths), is not the half-wavelength ground state. Thus, at earlier times a larger slab may well have a scattered light wave number which may initially correspond to a state with three half wavelengths in the slab, two half wavelengths in the slab (or perhaps even more for longer plasma slabs than those we have studied). In the cases where we found that we began with a mode above the ground state, we have seen the plasma scattering mode make transition(s) to lower modes, finishing up in the ground state. There are, of course, only very slight changes in the output frequency, since the system is very close to the plasma or cut-off frequency. Resolving these changes would require more sophisticated frequency detection techniques than simple windowed Fourier transform over time.

The reasons for this behavior are not easy to examine in detail because the interaction strength with the KEEN waves has no good analytical model to date, so there is (as yet) no basic theory model to which one can go for understanding. However, other interactions (such as SRS or SBS) which are well understood show that the growth rate tends to increase with the product of the electromagnetic scattered wave vector and the wave vector of the electrostatic mode. At the outset, therefore, it may well be quite normal that with longer slabs one begins with an electromagnetic scattering mode somewhat above the ground-state half-wavelength mode. Then, with time, the system evolves towards the lowest mode. This said, the detailed study of this effect, while perhaps of interest in itself, would require a great deal of numerical study in order to be able to quantify it and so this topic is not pursued further here.

VII. CONCLUSION

The basic mechanism has been demonstrated to account for a puzzling scattering instability in a plasma slab, involving an electrostatic wave at frequencies well below the plasma frequency, in what is sometimes termed "the spectral gap region," where no wave should occur. This wave was first seen in simulation using a PIC code by Nikolic, Skoric, Ishiguro and Sato [1] and although linked to phenomena discussed by Montgomery *et al.* [2] and by Rose *et al.* [3], it proves to be an example of a KEEN wave, a phenomenon previously treated by Afeyan *et al.* [10].

In systematic simulation studies of this scheme, we varied the characteristics of the SKSS instability: the ratio of the electron density to the critical density, the plasma edge scale length, and the plasma cavity width. Our investigation reveals that it is the radiating plasma cavity which determines the resonance conditions by imposing discrete values (multiples of the half-wavelength) for the wave number of the confined electromagnetic daughter wave. We have shown that in the relevant case of a plasma slab, it is the wave number selectivity of a different pseudomode (discussed here) a resonance of the plasma slab's radiating pseudocavity spectrum, that determines the frequency (very near the plasma frequency) and wave number of the scattered electromagnetic wave in the plasma (a few half wavelengths fit into the large plasma slab).

This parametric instability depends strongly on the boundary conditions (which, of course, are nonperiodic here) and in particular on the plasma slab thickness since the scattered mode (confined inside the cavity) is found to have one or more half wavelengths going down eventually to one half wavelength in the asymptotic phase corresponding to the ground state. This electromagnetic scattered mode, starting with an integer number of half wavelengths at the beginning of the simulation, evolves toward the lowest order ($n=1$) in the asymptotic state. This model also qualitatively explains why we have $\omega_s \simeq \omega_p \langle \gamma^{-1} \rangle^{1/2}$ provided that the plasma slab width is large enough so that the associated lower modes have small wave numbers ($\ll \omega_p \langle \gamma^{-1} \rangle^{1/2}/c$).

It is the beating of this slab pseudomode with the pump which will define the scattering frequency resonance and the KEEN frequency of about $\omega_0 - \omega_p \langle \gamma^{-1} \rangle^{1/2}$. Thus this mode combined with the pump wave produces a strong three-wave instability, using as the third mode, the KEEN waves which are nonresonant and intrinsically nonlinear. For sufficiently hot plasma slabs we have demonstrated the possibility of strong growth of this new parametric instability.

Although the plasma slab problem is now better understood, it remains to understand further how these KEEN waves might behave in realistically inhomogeneous plasmas, when driven up by spatially localized and temporally limited ponderomotive drivers.

From a numerical point of view, we have used a significantly different version of a semi-Lagrangian and relativistic Vlasov model using fixed (Eulerian) grids. However, much effort is still consumed in large regions of phase space which are unimportant because the particle density there is very low. We may hope that very important progress is be expected from new adaptive time-dependent grids with small mesh sizes in the nonzero regions and large mesh sizes for the sparse region. If successful, this will open new perspectives in the study of ultra-high and ultra-short laser-plasma interaction for inertial fusion.

ACKNOWLEDGMENTS

The authors gratefully acknowledge useful discussions with B. Afeyan, M. Passoni, and M. Lontano and also acknowledge the IDRIS Center for Computer Time Allocation on the NEC-SX5 computer.

[1] L. Nikolic, M. M. Skoric, S. Ishiguro, and T. Sato, Phys. Rev. E **66**, 036404 (2002).
[2] D. S. Montgomery, R. J. Focia, H. A. Rose, D. A. Russell, J. A. Cobble, J. C. Fernandez, and R. P. Johnson, Phys. Rev. Lett. **87**, 155001 (2001); see also Phys. Plasmas **5**, 2311 (2002).
[3] H. A. Rose and D. A. Russell, Phys. Plasmas **8**, 4784 (2001).
[4] I. B. Bernstein, J. M. Greene, and M. D. Kruskal, Phys. Rev. **108**, 546 (1957).
[5] F. Hohl, Phys. Fluids **12**, 230 (1969); see also J. P. Doremus, U. Finzi, J. Holec, and M. R. Feix, *ibid.* **16**, 189 (1974).
[6] J. L. Schwarzmeier, H. R. Lewis, B. Abraham-Schrauner, and K. R. Symon, Phys. Fluids **22**, 1747 (1979).
[7] A. Ghizzo, B. Izrar, P. Bertrand, E. Fijalkow, M. R. Feix, and M. Shoucri, Phys. Fluids **31**, 72 (1988); see also G. Manfredi and P. Bertrand, Phys. Plasmas **7**, 2425 (2000).
[8] H. Schamel, Phys. Plasmas **7**, 4831 (2000).
[9] J. P. Holloway and J. J. Dorning, Phys. Rev. A **44**, 3856 (1991).
[10] B. Afeyan, K. Won, V. Savchenko, T. W. Johnston, A. Ghizzo, and P. Bertrand, in *Proceedings of the Third International Conference on Inertial Fusion Sciences and Applications M034, Monterey, California, 2003*, edited by B. Hammel, D. Meyerhofer, J. Meyer-ter-Vehn, and H. Azechi (American Nuclear Society, LaGrange Park, IL, 2004), p. 213.
[11] Q. L. Dong, Z. M. Sheng, M. Y. Yu, and J. Zhang, Phys. Rev. E **68**, 026408 (2003).
[12] F. Huot, A. Ghizzo, P. Bertrand, E. Sonnendrucker, and O. Coulaud, J. Comput. Phys. **185**, 512 (2003); IEEE Trans. Plasma Sci. **28**, 1209 (2000).
[13] P. Bertrand, A. Ghizzo, T. W. Johnston, E. Fijalkow, and M. R. Feix, Phys. Fluids B **B2**, 1028 (1990); T. W. Johnston, P. Bertrand, A. Ghizzo, M. Shoucri, E. Fijalkow, and M. R. Feix, *ibid.* **B4**, 2523 (1992); A. Ghizzo, P. Bertrand, J. Lebas, T. W. Johnston, and M. Shoucri, J. Comput. Phys. **8**, 356 (1995); Phys. Plasmas **5**, 4041 (1998).